RSC Advances

RSC Publishing

COMMUNICATION

View Article Online
View Journal | View Issue

Benzo[1,2-*b*:4,5-*b*′]difuran-based sensitizers for dye-sensitized solar cells†

Cite this: *RSC Adv.*, 2013, **3**, 19798

Received 15th July 2013
Accepted 12th August 2013

DOI: 10.1039/c3ra43669a

www.rsc.org/advances

Hui Li,[a] Chenyi Yi,[b] Sofiane Moussi,‡[c] Shi-Xia Liu,*[a] Claude Daul,[c] Michael Grätzel*[b] and Silvio Decurtins[a]

Two BDF-based organic sensitizers, as first examples for their use in dye-sensitized solar cells, are prepared and characterized. They yield promising power conversion efficiencies of up to 5.5% and high open circuit voltages up to 0.82 V. This work demonstrates that the BDF chromophore acts as an effective donor in organic sensitizers.

Dye-sensitized solar cells (DSSCs) as low cost alternatives to traditional photovoltaics have attracted the interest of scientists from different disciplines, and their overall performances developed very rapidly day by day.[1–5] Despite the great achievement of Ru(II)-based dyes showing a power conversion efficiency (PCE) of up to 12%,[5] much effort has been devoted to the attainment of metal-free organic dyes due to their low cost, ease of synthesis, structural diversity, and remarkably high optical extinction coefficients. Consequently, a large number of organic dyes, typically with a donor–π–acceptor (D–π–A) configuration, have extensively been investigated for DSSCs.[1–7] In practice, a judicious variation of the molecular architectures of the donor fragments as well as of the π-linkers between the donor and acceptor fragments of the dyes, has been the most popular strategy to tailor the frontier orbital energy levels, which finally leads to the formation of dyes with broad and intense optical absorption patterns.[8,9] Various molecular scaffolds such as triarylamine, carbazole, porphyrin, and indoline, have been used as attractive components in organic sensitizers. To the best of our knowledge, within this context there has been no report on systems featuring a benzo[1,2-*b*:4,5-*b*′]difuran (BDF) chromophore.

BDFs have proven to be excellent components in organic field-effect transistors (OFETs) and organic light-emitting diodes (OLEDs) by virtue of their π-type semiconductor characteristics, intrinsic optical properties and high hole mobility.[10,11] It is noteworthy that their cationic radicals formed by a one-electron oxidation, show an intriguing stability.[12,13] Thus, the BDF-based dyes are expected to have an enhanced stability in photo-induced electron transfer processes from the dyes to TiO_2. For an efficient design of conjugated D–π–A dyes, one of the key issues relates to the synthesis of properly functionalized BDFs, which has rarely been exploited due to the associated synthetic challenges. In previous studies we have developed efficient synthetic routes to fully functionalized BDF derivatives.[12–16] On this basis, we have been able to obtain two π-conjugated dyes (Fig. 1) that feature the BDF donor linked to one (**Dye-1**) and two (**Dye-2**) standard cyanoacrylic acid acceptors. To date, studies on the effect of the number and the positioning of a cyanoacrylic acid anchoring group on the cell performance are quite scarce.[17,18] We report herein the synthesis and DSSC performance of **Dye-1** and **Dye-2**. This work elaborates on the impact of the number of cyanoacrylic acid anchoring groups on the overall efficiencies of solar cells based on BDF donors.

As illustrated in Scheme 1, two new dyes were synthesized in good yields as red solids *via* a Knoevenagel reaction with cyanoacetic acid. The corresponding aldehyde precursor **II** was readily obtained from **I**[14] in 74% yield by reaction with one equivalent of 4-bromobenzaldehyde under standard Sonogashira conditions. Similarly, a Sonogashira reaction of **III**[12,13] with 4-ethynylbenzaldehyde was accomplished to afford the dialdehyde **IV**.[19] The target dyes and intermediate compounds have been fully characterized. Their NMR spectroscopic and

[a]*Departement für Chemie und Biochemie, Universität Bern, Freiestrasse 3, CH-3012 Bern, Switzerland. E-mail: liu@iac.unibe.ch; Fax: +41 31 631 43 99; Tel: +41 31 631 42 96*

[b]*Laboratory of Photonics and Interfaces, Institute of Chemical Science and Engineering, École Polytechnique Fédérale de Lausanne (EPFL), Station 6, CH-1050 Lausanne, Switzerland. E-mail: michael.graetzel@epfl.ch; Fax: +41 21 693 61 00; Tel: +41 21 693 31 12*

[c]*Computational Chemistry Lab, Department of Chemistry, University of Fribourg, Ch. du Musée 9, CH-1700 Fribourg, Switzerland*

† Electronic supplementary information (ESI) available: Experimental procedure and characterization data for **Dye-1** and **Dye-2**, copies of their ^{1}H and ^{13}C NMR spectra, their detailed DFT calculations as well as their optical spectra on TiO_2. See DOI: 10.1039/c3ra43669a

‡ Present address: Faculté de Chimie, Université des Sciences et de la Tecnologie Houarie Boumedienne, laboratoire de Chimie Théorique Computationnelle et photonique, Bebezzouar Alger, Algeria.

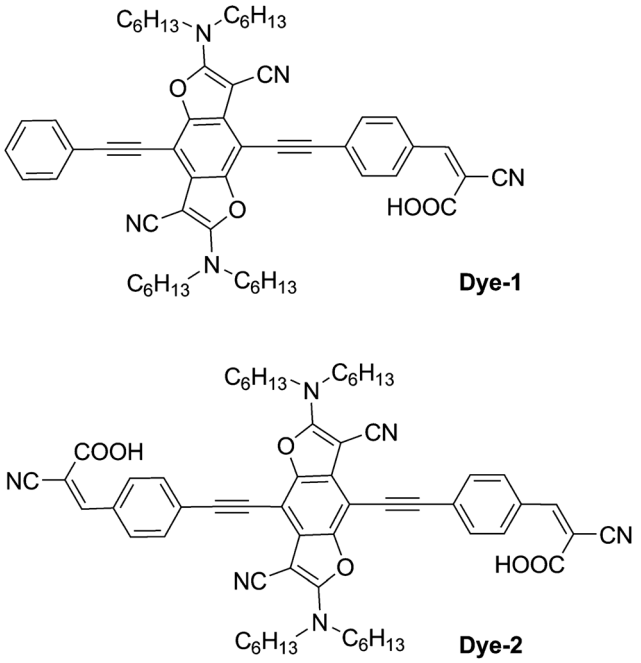

Fig. 1 Chemical structures of the synthesized dyes.

mass spectrometric data are consistent with their proposed structures. Both dyes are polycrystalline as confirmed by the powder X-ray diffraction patterns (see ESI†).

The optical and redox properties of the new dyes are listed in Table 1. Their electrochemical properties in $CHCl_3$ were investigated by cyclic voltammetry (CV). **Dye-1** undergoes two reversible one-electron oxidations at 0.36 and 0.63 V for the successive generation of the BDF^{+} radical cation and the BDF^{2+} dication.[12–16] In contrast, in the case of **Dye-2** these processes are not electrochemically fully reversible (see ESI†). This compound shows two distorted anodic peaks with $E^{1}_{pa} = 0.51$ V and $E^{2}_{pa} = 0.77$ V, and two successive cathodic peaks at $E^{1}_{pc} = 0.33$ V and $E^{2}_{pc} = 0.43$ V. This observation is indicative of an electron-transfer reaction, most probably coupled with a complex sequence of chemical follow-up processes. Upon the addition of one more cyanoacrylic acid anchoring group, the first oxidation potential is substantially positive-shifted, which reflects the electronic interaction between D and A within these dyes. The first oxidation potential in both cases is more positive than the Co(II)/Co(III) redox couple in use, ensuring efficient regeneration of the oxidized dye. Moreover, the HOMO and LUMO energy levels of both dyes were estimated according to the spectral analyses and the CV data (Table 1). Their relatively low-lying HOMO energy levels are expected to reveal good air stability and a high open circuit voltage (V_{oc}) in the DSSC device. Compared to **Dye-1**, the HOMO and LUMO levels of **Dye-2** are energetically lowered due to the strong electron-withdrawing effect of two cyanoacrylic acid anchoring groups.

Density-functional theory (DFT) calculations for both dyes using the Coulomb Attenuated Methods at the B3LYP 6-31G(d,p) level of the theory, support the directional movement of charge upon photoexcitation (for details, see ESI†). As expected, the HOMO and LUMO of **Dye-1** and **Dye-2** are mainly located on the BDF and 2-cyano-3-(4-ethynylphenyl)acrylic acid moieties, respectively. An energetic stabilization of the HOMO when going from **Dye-1** (−5.09 eV) to **Dye-2** (−5.11 eV) is predicted, which is in line with the increase of the oxidation potential from **Dye-1** to **Dye-2**; see Table 1.

The electronic spectra of the red colored **Dye-1** and **Dye-2**, recorded in THF solution (see ESI†), show intense optical absorptions over the UV-vis spectral part with absorption onset energies at about 17 900 cm^{-1} (559 nm) and 17 100 cm^{-1} (585 nm), respectively. As expected, both of them exhibit a quite similar absorption pattern. Based on the detailed spectral

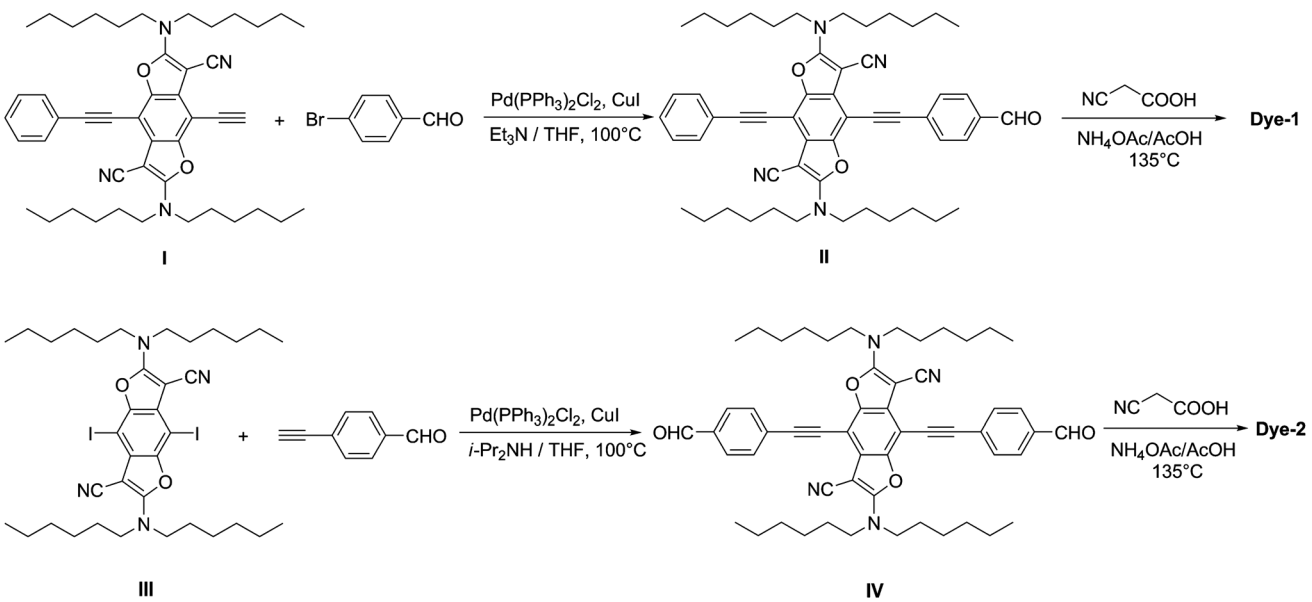

Scheme 1 Synthesis of **Dye-1** and **Dye-2**.

Table 1 Optical and electrochemical data, HOMO and LUMO energy levels, and photovoltaic parameters of **Dye-1** and **Dye-2** after optimization

Dye	λ_{abs}^{max} (nm) (ε_{max} (10^4 M^{-1} cm^{-1}))	λ_{em}^{max} (nm)	$E_{g,opt}$ [a] (eV)	E^b (V)	HOMO[e] (eV)	LUMO[f] (eV)	J_{sc}[g] (mA cm^{-2})	V_{oc}[g] (mV)	FF[g]	PCE[g] (%)
Dye-1	477 (1.6)	497	2.22	0.36[c]	−5.09	−2.87	8.7	820	0.77	5.5
Dye-2	516 (2.1)	—	2.12	0.51[d]	−5.11	−2.99	6.1	750	0.81	3.8

[a] Optical band gap is estimated from UV-vis absorption onset. [b] The redox potentials *vs.* Fc^+/Fc were recorded in $CHCl_3$–Bu_4NPF_6 (0.1 M) solution. [c] It corresponds to half-wave oxidation potential $E_{1/2}{}^1$. [d] It corresponds to an anodic peak $E_{pa}{}^1$. [e] HOMO level is calculated from the onset of the first oxidation potential in cyclic voltammetry, according to the equation $E_{HOMO} = [-e(E_{onset} + 4.8)]$ eV, where 4.8 eV is the energy level of ferrocene below the vacuum level. [f] LUMO level is estimated according to the equation $E_{LUMO} = [E_{g,opt} + E_{HOMO}]$ eV. [g] The cells were tested with a solution of dye (0.1 mM) in the presence of CDCA using a [Co(II/III)(bpy)$_3$] electrolyte under standard air mass 1.5 and simulated sunlight at 1000 W m^{-2} intensity.

analysis of the related BDF derivative with pending 4-ethynylpyridine groups[13] and DFT calculations, the main characteristics of the electronic transitions can be explained. Firstly, at low wavelength a strong and broad absorption band appears around 20 960 cm^{-1} (477 nm) for **Dye-1** and 19 380 cm^{-1} (516 nm) for **Dye-2**, which can only be observed in such π-extended chromophores and is attributed to intramolecular π–π* charge-transfer (ICT) transitions from the BDF unit (HOMO, HOMO − 1 and HOMO − 2) to the 2-cyano-3-(4-ethynylphenyl)acrylic acid unit(s) (LUMO, LUMO + 1 and LUMO + 2) (for the relevant orbitals, see ESI†). The intense absorptions between 23 000 cm^{-1} (435 nm) and 31 000 cm^{-1} (323 nm) originate to a larger extent from BDF-based π–π* transitions. Compared to **Dye-1**, the red-shift of 1580 cm^{-1} and an increase in the molar extinction coefficient (ε) for the ICT band in **Dye-2** are attributed to the extension of the π-conjugation of the BDF unit.

The absorption spectra of **Dye-1** and **Dye-2** adsorbed on a TiO_2 film (see ESI†) show that the ICT absorption bands, related to those in THF, are red-shifted by 11 nm and blue-shifted by 12 nm, respectively.

Despite similar optical and redox properties for the two dyes, in the presence of a prototype coabsorbent, chenodeoxycholic acid (CDCA), which prevents dye aggregation on the TiO_2 surface, DSSC experiments revealed an enhanced performance of the **Dye-1**-based cells relative to **Dye-2**-based cells. The discrepancy in their cell performances can be rationalized by the incident photon-to-current conversion efficiency (IPCE) spectra depicted in Fig. 2. The IPCE depends on the light-harvesting efficiency, the net charge injection efficiency, and the electron collection efficiency.[20] The integrated IPCE values between 400 nm and 540 nm exceed 60% for **Dye-1**, and they are higher than those for **Dye-2** by a factor of 1.2. Both the short-circuit photocurrent density (J_{sc}) and the power conversion efficiency (PCE) values for **Dye-1** (Table 1, Fig. 2) are consistently higher than those for **Dye-2** by a factor of 1.4. It can be therefore deduced that the presence of four hexyl groups prevents the leakage of electrons from TiO_2 to the electrolyte/the oxidized dye, and thus effectively suppresses the recombination processes, leading to the large FF (0.81 and 0.77) and high V_{oc} values. As a result, the PCE values decrease progressively from 5.5% (**Dye-1**) to 3.8% (**Dye-2**). Based on all these observations and previously reported results in other DSSCs,[17,18,20,21] the differences between **Dye-1** and **Dye-2** in IPCE behavior are most likely ascribed to their net injection efficiencies.

In conclusion, we have presented a new type of dye sensitizers endowed with a BDF π-conducting group for DSSCs, namely, fluorescent **Dye-1** and non-emissive **Dye-2** with one and two cyanoacrylic acid anchoring groups, respectively. For the first time, BDF-sensitized DSSCs are described, showing PCEs of up to 5.5% in the presence of the coabsorbent CDCA. Detailed kinetic studies of DSSCs based on these two dyes will be carried out to determine their quantum yields for electron injection. Also a study on the structural modification of the BDF dyes capable of extending the spectral response to the long wavelength region and further enhancing the DSSC performance, is currently underway.

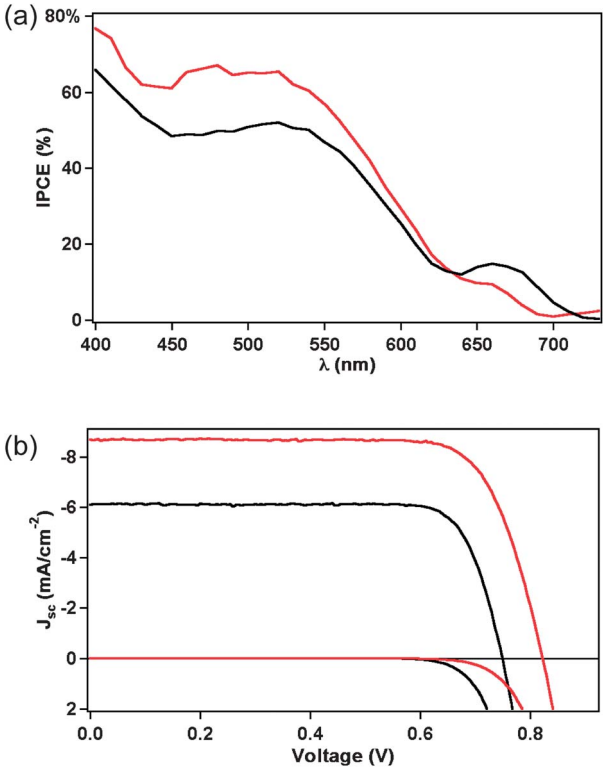

Fig. 2 Photovoltaic performance of two BDF-based dyes in the presence of CDCA. (a) Photocurrent action spectra for **Dye-1** (red) and **Dye-2** (black), showing the IPCE as a function of excitation wavelength. (b) Photocurrent density (J) as a function of voltage (V) for **Dye-1** (red) and **Dye-2** (black) measured under standard air mass 1.5 and simulated sunlight at 1000 W m^{-2} intensity.

This work was funded by the Swiss National Science Foundation (Grant no. 200020-130266 and 200021-147143), the Sino Swiss Science and Technology Cooperation and the EC FP7 ITN 'FUNMOLS' project no. 212942.

Notes and references

1 Y. Wu and W. Zhu, *Chem. Soc. Rev.*, 2013, **42**, 2039.
2 Z. Ning, Y. Fu and H. Tian, *Energy Environ. Sci.*, 2010, **3**, 1170.
3 J. N. Clifford, E. Martinez-Ferrero, A. Viterisi and E. Palomares, *Chem. Soc. Rev.*, 2011, **40**, 1635.
4 A. Hagfeldt, G. Boschloo, L. Sun, L. Kloo and H. Pettersson, *Chem. Rev.*, 2010, **110**, 6595.
5 A. Mishra, M. K. Fischer and P. Baeuerle, *Angew. Chem., Int. Ed.*, 2009, **48**, 2474.
6 L.-L. Li and E. W.-G. Diau, *Chem. Soc. Rev.*, 2013, **42**, 291.
7 Z. Ning and H. Tian, *Chem. Commun.*, 2009, 5483.
8 A. Yella, H. W. Lee, H. N. Tsao, C. Y. Yi, A. K. Chandiran, M. K. Nazeeruddin, E. W. G. Diau, C. Y. Yeh, S. M. Zakeeruddin and M. Graetzel, *Science*, 2011, **334**, 629.
9 H. N. Tsao, C. Yi, T. Moehl, J. H. Yum, S. M. Zakeeruddin, M. K. Nazeeruddin and M. Graetzel, *ChemSusChem*, 2011, **4**, 591.
10 H. Tsuji, C. Mitsui, L. Ilies, Y. Sato and E. Nakamura, *J. Am. Chem. Soc.*, 2007, **129**, 11902.
11 L. Huo, L. Ye, Y. Wu, Z. Li, X. Guo, M. Zhang, S. Zhang and J. Hou, *Macromolecules*, 2012, **45**, 6923.
12 S. Keller, C. Yi, C. Li, S.-X. Liu, C. Blum, G. Frei, O. Sereda, A. Neels, T. Wandlowski and S. Decurtins, *Org. Biomol. Chem.*, 2011, **9**, 6410.
13 C. Yi, C. Blum, M. Lehmann, S. Keller, S.-X. Liu, G. Frei, A. Neels, J. Hauser, S. Schuerch and S. Decurtins, *J. Org. Chem.*, 2010, **75**, 3350.
14 H. Li, J. Ding, S. Chen, C. Beyer, S.-X. Liu, H.-A. Wagenknecht, A. Hauser and S. Decurtins, *Chem.–Eur. J.*, 2013, **19**, 6459.
15 H. Li, P. Tang, Y. Zhao, S.-X. Liu, Y. Aeschi, L. Deng, J. Braun, B. Zhao, Y. Liu, S. Tan, W. Meier and S. Decurtins, *J. Polym. Sci., Part A: Polym. Chem.*, 2012, **50**, 2935.
16 H. Li, P. Jiang, C. Yi, C. Li, S.-X. Liu, S. Tan, B. Zhao, J. Braun, W. Meier, T. Wandlowski and S. Decurtins, *Macromolecules*, 2010, **43**, 8058.
17 M. J. Cho, S. S. Park, Y. S. Yang, J. H. Kim and D. H. Choi, *Synth. Met.*, 2010, **160**, 1754.
18 A. S. Hart, K. C. Chandra Bikram, N. K. Subbaiyan, P. A. Karr and F. D'Souza, *ACS Appl. Mater. Interfaces*, 2012, **4**, 5813.
19 H. Li, C. Schubert, P. O. Dral, R. D. Costa, A. La Rosa, J. Thüring, S.-X. Liu, C. Yi, S. Filippone, N. Martín, S. Decurtins, T. Clark and D. M. Guldi, *ChemPhysChem*, 2013, DOI: 10.1002/cphc.201300378.
20 M. K. Nazeeruddin, A. Kay, I. Rodicio, R. Humphry-Baker, E. Mueller, P. Liska, N. Vlachopoulos and M. Graetzel, *J. Am. Chem. Soc.*, 1993, **115**, 6382.
21 W. M. Campbell, A. K. Burrell, D. L. Officer and K. W. Jolley, *Coord. Chem. Rev.*, 2004, **248**, 1363.